4th International Conference on Water Resources and Arid Environments (ICWRAE 4): 781-792
5-8 December 2010, Riyadh, Saudi Arabia

Effect of Vegetation on Soil Moisture Retrieval from *Ers-2 Sar* Images

S. Said[1], U.C. Kothyari[2] and M.K. Arora[2]

[1]Department of Civil Engineering, Jamia Millia Islamia, New Delhi, India
[2]Department of Civil Engineering, Indian Institute of Technology Roorkee, Roorkee, India

Abstract: It is known that the relation between crop covered soil moisture and backscatter coefficient is highly perturbed by a number of factors such as topography of the terrain, vegetation density and variations in small-scale surface roughness. The effect of these factors needs to be minimized in order to accurately establish the relationship between backscatter coefficient and crop covered volumetric soil moisture. The aim of this study is to map soil moisture from *ERS-2 SAR* images by minimizing the effect of vegetation on the backscatter coefficient. For minimizing the crop effect on soil moisture, it is important to know the impact of individual crop descriptors (*i.e.*, crop height; *h*, Leaf Area Index; *LAI*, Plant Water Content; *PWC*) on backscattering coefficient. For this purpose, a detailed analysis has been carried out to identify the prominent crop descriptor and to minimize its effect on soil moisture estimation. Semi-empirical water cloud model was used to eliminate the vegetation effects on backscatter coefficient. Three images of three different dates (*i.e.*, 28th July 2003, 29th March 2004 and 3rd May 2004) corresponding to three markedly different seasons were acquired over a typical river catchment in India. The results showed that the water cloud model based on *LAI* as the canopy descriptor was able to estimate crop covered backscatter coefficient more accurately than the models based on either of the remaining two crop descriptors. Once the crop covered backscatter coefficient was determined, a nonlinear least square method (*LSM*) was implemented to retrieve the volumetric soil moisture. A significantly high correlation (coefficient of determination, R^2 • 0.94) between the retrieved soil moisture and the corresponding observed in-situ soil moisture for barren land as well as crop covered surfaces was obtained. Subsequently, soil moisture maps were generated from three images individually to depict the spatial distribution of soil moisture during the three seasons. The estimated spatial distribution of the soil moisture was also compared closely with the in-situ observations.

Key words: Backscatter coefficient • Microwave remote sensing • *Rms* surface roughness • Water cloud model

INTRODUCTION

Ground surface soil moisture is the key parameter that plays a significant role in partitioning of precipitation into runoff and infiltration processes and is considered as a key input variable in a number of scientific studies in hydrology, meteorology and agriculture. Knowledge of spatial distribution of soil moisture in a region in near real time is therefore needed for

- Forecasting of river flows resulting due to rainfall during storm events
- Planning, designing and scheduling of irrigation systems
- Soil conservation studies

Conventionally, soil moisture has been directly measured at sampled locations using gravimetric or other such methods. Fortunately, microwave radar images have the potential of quantifying the spatial distribution of volumetric soil moisture. This is due to the fact that microwaves penetrate into the soils with vegetation and high surface roughness. However, accurate retrieval of soil moisture from *RADAR* images is not simple since the backscatter coefficient, σ° (*i.e.*, the pixel wise *RADAR* data,) is strongly influenced by the surface as well as sensor related parameters. The surface related parameters include dielectric constant, topography, type of vegetation and surface roughness whereas sensor related parameters include incidence angle, polarization and frequency. Variation of the soil moisture over a depth up

Corresponding Author: S. Said, Department of Civil Engineering, Jamia Millia Islamia, New Delhi, India.
E-mail: saif _said@rediffmail.com.

to 5 cm below the general ground surface is possible to be retrieved using the active microwave technology Ulaby *et al* [1].

The effect of surface related parameters such as topography and vegetation on backscatter coefficient can be studied via a number of modeling approaches. For minimizing the effect of vegetation, a semi-empirical water cloud model, developed by Attema and Ulaby, [2] and later modified by various authors [1, 3, 4-7] may be used. The water cloud model defines the total backscatter coefficient recorded by the sensor over vegetated surfaces as an incoherent sum of the contributions of vegetation and soil [8]. In this model, the canopy is usually represented as a set of detailed descriptors such as plant density per square meter, size of leaf and its orientation etc [9], which makes the model complex and difficult to understand. Recent experimental studies [6, 10-15] sufficiently demonstrate the application of water cloud model. Roo *et al* [16] used a very large number of vegetation parameters (*e.g.*, shape of canopy, stem thickness, leaf size and orientation, leaf moisture and plant density per square meter) in order to reduce the effect of vegetation on observed backscatter coefficient. Alternatively, the bulk variables such as *LAI, PWC* and *h* may also be used as surrogates of detail descriptors in the model, as has been demonstrated by several studies [8, 17-21].

The aim of the present study is to further simplify the procedures of estimating soil moisture by identifying a single canopy descriptor for use in the water cloud model so as to minimize the effect of vegetation from the crop covered backscatter coefficient. A comparative study is also presented on the use of any of the three major descriptors of vegetation namely *LAI*, *PWC* and *h* or their combination in retrieval of soil moisture from *ERS-2 SAR* data.

Study Area: The study area belongs to a catchment of river Solani (a tributary of the river Ganges) around Roorkee town (between geographical coordinates 78.03°E, 30.00°N and 77.48°E, 29.45°N), India. The area is relatively flat with a maximum slope of 4°. The moisture conditions in the area were very different during the three seasons in which the *SAR* images were acquired. One of these (*i.e.* the start of autumn season) had fairly good amount of rainfall, which resulted in an average value of relative humidity in the atmosphere was observed to be 65% to 70% in the region. During this period, the area comprised of mixed vegetation consisting of grassland, sugarcane, cherry and rice. Crops were at their mature stage leading to a variation in both surface roughness and the amount of moisture within the field. Next of the seasons was end of spring that had meager rainfall and humidity less than 50%. The last one being beginning of the summer season had effectively no rainfall and humidity less than 40%. During the spring and summer seasons, the area was dominated mainly by four land cover classes - barren land, grassland, sugarcane and wheat.

Experimental Datasets

Remote Sensing Data: Three *ERS-2 SAR,* C band images (5.3 GHz frequency and *VV* polarization) at spatial resolution of ~12.5 m acquired on 28th July 2003 (start of autumn season), 29th March 2004 (end of spring season) and 3rd May 2004 (start of summer season), were procured. Two images from Linear Imaging and Self Scanning sensors (*LISS II* and *LISS III*) of dates 23rd June 2002 (autumn season) and 12th March 2004 (spring season) on-board Indian Remote Sensing (*IRS*) satellite providing data at spatial resolution of ~ 36 m and ~ 23.5 m were also utilized to produce land cover classification of the study area so as to identify the class allocation of the sampled pixels in *SAR* data pertaining to three different seasons.

Field Data: Surface roughness height, plant and leaf samples for estimating *LAI* and *PWC* and the plant heights were measured in the field. Soil samples at a large number of selected locations were collected concurrent to the dates of the satellite pass to estimate the volumetric soil moisture using field based conventional gravimetric method. At each location, five soil samples were collected within a radial distance of 20 m and the average values of soil moisture at a particular location were considered for establishing their relationships with the backscatter coefficient. The total number of sampling locations was 112, 102 and 102 respectively corresponding to the three dates on which satellite data were acquired. Out of the total samples, 80% were used for model calibration and the rest were utilised for model validation (*i.e.*, the accuracy of soil moisture maps were examined by validation data). The soil samples were collected from both vegetative and barren land surfaces up to 5 cm thick soil layer beneath the top surface. Global Positioning System (*GPS)* surveys were conducted to determine the coordinates of 380 locations, which in conjunction with topographical map at scale of 1:50,000 (Survey of India map sheet number 53 G/13) were used for the generation of a Digital Elevation Model (*DEM*) of the study area.

A surface roughness profiler was also designed and developed in-house to measure the *rms* surface roughness heights, which were also used subsequently for computation of the backscatter coefficient using

Dubois model [22]. The profiler has a base length of 85 cm with 69 vertical needles of height 70 cm each placed at an equal interval of 10 mm. The profiler was placed at 3 to 4 locations around each sampling point in the field to collect the data pertaining to the surface roughness. The measurements were taken and averaged for that location. The *rms* heights (*s*) of the surface were computed as [23]:

$$s = \sqrt{\frac{1}{n}\sum_{x=1}^{n-1}\left[S(x) - \overline{S}(x)\right]^2} \quad (1)$$

Where, *S(x)* is the surface height at a point x in the surface profile, $\overline{S}(x)$ is the average height of the surface profile and *n* is the total number of points (vertical rods) along the abscissa.

Methodology for Soil Moisture Estimation Using *ERS-2 SAR* Image: Keeping in view the objective of the present study, the following methodology was adopted,

- Geo-referencing of *SAR* images.
- Speckle reduction in *SAR* images.
- Computation of backscatter coefficient and the local incidence angle.
- Generation of Digital Elevation Model (*DEM*), slope and aspect maps.
- Land cover classification from *LISS II* and *III* data.
- Assessment of the effect of vegetation on crop covered backscatter coefficient;
- Soil moisture retrieval through non linear least squares method
- Generation of soil moisture maps.
- Model validation

Geo-referencing of *ERS-2 SAR* Images: Three *SAR* images were geo-referenced with respect to geographic coordinates using traditional feature based registration technique by selecting sufficient number of ground control points (*GCP*) and applying first-order polynomial transformation followed with nearest neighbour re-sampling. The geo-referencing of *SAR* images enabled the identification of soil sampling locations on images so as to extract the *DN* values at corresponding locations, which were later required for computing σ°.

Speckle Reduction in *SAR* Images: The effect of speckles in the geo-referenced *SAR* images was reduced by the application of widely used spatial filter, namely Lee-sigma filter. The Lee-Sigma filter utilizes the statistical distribution of the *DN* values within the moving kernel to estimate the value of the pixel of interest in the image data. This filter is based on the probability of a Gaussian distribution and assumes that 95.5% of random samples are within a 2 standard deviation range [24]. The speckle-adjusted geo-referenced images were used to extract the *DN* values of pixels corresponding to soil sampling locations.

Computation of Backscatter Coefficient and Local Incidence Angle: Backscatter coefficient and the local incidence angle of pixels corresponding to each sampling location were determined on the basis of the algorithm proposed by Laur *et al*. [25]. Accordingly, the relation between the backscatter coefficient as a function of *DN* of the pixel and the incidence angle is given by:

$$\sigma^\circ = \left[\frac{1}{N}\cdot\sum_{ij=1}^{ij=N} DN_{ij}^2\right]\cdot\frac{1}{K}\cdot\frac{\sin\alpha_i}{\sin\alpha_{ref}} \quad (2)$$

Where, *N* is the number of pixels within the area of interest (*i.e.*, the distributed target). DN_{ij} is the digital number corresponding to the pixel at location (*i, j*). α_i and α_{ref} are the local and average or mid range incidence angles respectively. The value of α_{ref} for *SAR* sensor and *K* is the calibration constant. The values of α_{ref} and K, as obtained from the sensor's ephemeris record are 23° and 889201.00 respectively.

The local incidence angle α_i for a pixel at range location *i* may be computed as:

$$\cos\alpha_i = \frac{(R_T + H)^2 - R_i^2 - R_T^2}{2R_iR_T} \quad (3)$$

Where, R_T is the radius of the Earth at the first position of satellite, *H* is the altitude of *ERS-2* satellite and R_i is the slant range to a pixel at location *i*. The σ° computed from Eq. (2), by substituting the values of local incidence angle obtained from Eq. (3) has been termed as direct backscatter coefficient 'σ_D^0' as observed by the *SAR* sensor. The σ_D^0 were computed for all the sampling locations using Eqs. (2) and (3).

However, studies by several investigators [6, 10, 11, 13, 26] have shown that σ_D^0 is highly influenced by a number of factors that result in weakening of direct backscatter coefficient. Hence, before relating σ_D^0 with soil moisture, the effect of surface related parameters such as topography, surface roughness and vegetation cover on σ_D^0 must be estimated for accurate estimation of soil moisture.

Generation of *DEM*, Slope and Aspect Maps: The effect of topography must be accounted for on backscatter coefficient, since it causes the local incidence angle to be different from that assumed for a flat surface due to high spatial resolution of *SAR* images. The information about the topography of the study area was quantified by determining heights through Global Positioning Survey *(GPS*) surveys. The *GPS* derived heights along with latitude and longitude coordinates of 380 sampling locations formed the basis of generating a Digital Elevation Model (*DEM)*, which depicted the spatial distribution of topography of the area. The *DEM* was subsequently used to derive slope and aspect maps; a pertinent information to be input to the model to minimise the effect of topography on backscatter coefficient.

Land Cover Map: The land cover map is derived to know the extent of vegetative and non-vegetative cover (*i.e.*, barren land) in the study area. Two land cover maps of the study were prepared through classification of *LISS II* and *LISS III* images using the most widely used Maximum Likelihood Classifier (*MLC*). The land cover maps in the form of classified images are shown in Fig.1 (a, b). The pixel wise information about the land cover *i.e.*, type of vegetation and barren land) at soil sampling locations was obtained from these maps. This was a necessary input for the model in order to minimise the effect of vegetation on backscatter coefficient.

Assessing the Effect of Vegetation on Crop Covered Backscatter Coefficient: In areas with high topographic relief, radiometric variations are introduced in the *SAR* image. These variations are related to several parameters such as incidence angle, shadow, image foreshortening and image layover [27]. The slope map generated from *DEM* of the study area reveals a maximum slope of 4° only within this region. Thus, the area may be regarded as generally flat and it is, therefore, revealed that the effect of topography in this study area may be negligible.

To asses the effect of vegetation on crop covered backscatter coefficient, a number of approaches [1, 1, 2, 8, 16, 28-30] have been advocated. The basic approach for estimating soil backscatter coefficient underneath vegetation, used here, was based on the water cloud model [2]. In this model, the total backscatter coefficient recorded by the sensor over the vegetation is represented by the incoherent sum of the contributions of vegetation and soil. Vegetation component can be represented by bulk variables namely *LAI, PWC* and *h* as canopy descriptors. The water cloud model for a given incidence angle is represented as [8]:

$$\sigma^0_{canopy} = \sigma^0_{veg} + \gamma^2 \sigma^0_{soil} \quad (4)$$

$$\sigma^0_{veg} = AV_1 \cos\alpha_{ref}(1-\gamma^2) \quad (5)$$

$$\gamma^2 = \exp(\bullet\ 2V_2 B / \cos\alpha_{ref}) \quad (6)$$

and

$$\sigma^0_{soil} = C + Dm_v \quad (7)$$

Where, γ^2 is the two-way canopy transmitting factor. In Eq. (5) and (6), V_1 and V_2 are the canopy descriptors, A and B are coefficients that depend on type of vegetation. σ^0_{soil}, is the backscatter coefficient of the soil underneath vegetation which includes soil moisture and soil surface roughness, σ^0_{veg} is the backscatter due to vegetation only and σ^0_{canopy} is the total backscatter coefficient over the canopy as observed by the *SAR* sensor.

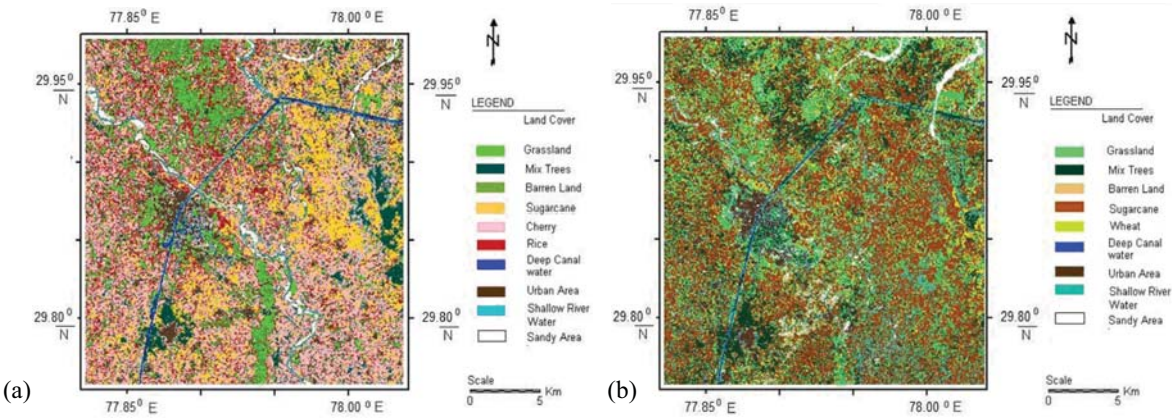

Fig. 1: Land cover maps of Solani river catchment prepared from (a) *LISS II* Image of date 23rd June 2002 (autumn season) and (b) *LISS III* image of date 12th March 2004 (spring season)

Although, any of the three canopy descriptors can be used to represent V_1 and V_2, a novel approach based on regression elimination has been proposed here to consider only single canopy descriptor to further simplify the water cloud model. To achieve this, three different scenarios each considering one canopy descriptor at a time were framed. This led to three models, given by:

a) Model 1 $V_1 = V_2 = LAI$ (8)
b) Model 2 $V_1 = V_2 = PWC$ (9)
c) Model 3 $V_1 = V_2 = h$ (10)

Model 1 uses *LAI*, defined as the one-sided green leaf area per unit ground area and characterizes the density of vegetation in accordance to the size of the leaf that actively participates in weakening of the backscatter coefficient over vegetation [29]. The *LAI* can be computed using the following relation,

$$LAI = N_a \times A_l \tag{11}$$

Where, N_a is the areal density of the scattering elements which was obtained from field measurements, A_l is the one sided area of the leaf determined by on-screen digitisation of leaves on their scanned photographs.

Model 2 uses *PWC* as the canopy descriptor, which is defined as the total amount of water (or moisture) present in the samples of plant leaves and stem. Since, dielectric properties of the vegetation are governed by *PWC*, plays a dominant part in attenuation processes of the backscatter coefficient [2]. *PWC* can be computed from:

$$PWC = \frac{W_f - W_d}{W_d} \tag{12}$$

Where, W_f and W_d are the freshly plucked and oven-dried weights of plant samples collected in the field.

Model 3 uses '*h*' as the canopy descriptor to minimize the vegetation influence on the backscatter coefficient. Plant heights (*h*) in meters were recorded in each vegetated covered area by using a surveyor's leveling staff.

Thus, *LAI, PWC and h* values were computed at sampling locations for different vegetation cover types under study and were used in Eqs. (4 to 7) to estimate the backscatter coefficient of the soil underneath vegetation cover (σ^0_{soil}) as:

$$\sigma^0_{soil} = \frac{\sigma^0_{canopy} - \sigma^0_{veg}}{\gamma^2} \tag{13}$$

After considering the effect of vegetation, another parameter that requires attention is the surface roughness and its effect on backscatter needs to be minimised. Therefore, an empirical model proposed by Dubois *et al*. [22] and given by Eq. (14) was utilized to estimate theoretical backscatter coefficient referred to as calculated backscatter coefficient σ^0_{cal}, of the soil over barren land. The Dubois model incorporates surface roughness, measured as *rms* heights of surface determined with the help of surface roughness profile and dielectric constant of the soil, represented by '*s*' and ε' respectively in the following equation:

$$\sigma^0_{cal} = 10^{-2.35} \frac{cos^3 \alpha_{ref}}{sin \alpha_{ref}} 10^{0.046 \tan \alpha_{ref} \varepsilon'} (ks \sin^3 \alpha_{ref})^{1.1} \lambda^{0.7} \tag{14}$$

Where, λ is the wavelength of the incident wave (λ=5.6 cm),ε' is the real part of dielectric constant of soil and *k* is the wave number, defined as $2\pi/\lambda$. The calculated backscatter coefficient (σ^0_{cal}), the backscatter coefficient as estimated from water cloud model (σ^0_{obss}) and the observed soil moisture ($m_{v_{obs}}$) obtained from gravimetric method as *a-priori* information for each sampling location were used as input to the nonlinear least squares solver objective function to retrieve the true soil moisture ($m_{v_{est}}$):

$$Minimize = \sum_{n_s=1}^{n_s} \left[\frac{1}{\eta^2_1} (\sigma^0_{obs} - \sigma^0_{cal})^2 + \frac{1}{\eta^2_2} (m_{v_{obs}} - m_{v_{est}})^2 \right] \tag{15}$$

Where, η_1 and η_2 are the standard deviations of σ^0_{obss} and $m_{v_{obs}}$. The function is optimised in an iterative manner with the aim to minimise the measurement errors in the observed data.

RESULTS AND DISCUSSION

The *DN* values of pixels in *SAR* images that correspond to the sampling locations in the field were extracted and were used to compute the backscatter coefficient ($\sigma°$) at each location *via* Eq. (2). These were termed as the direct backscatter coefficient (σ^0_D). The range of values (maximum and minimum) of σ^0_D α_i and observed soil moisture, m_v, for three seasons are given in

Table 1: Variance explained by the relation between σ_D^0 with m_v, Maximum (Max) and minimum (Min) values of σ_D^0, α_i and m_v for data of three seasons

				Backscatter coefficient σ_D^0 (dB)		Local incidence angle α_i (degrees)		Soil moisture m_v(%)		
S No.	*SAR* images	Land cover class	Total number of samples	Max	Min	Max	Min	Max	Min	R^2
1	Autumn season	Sugarcane	20	-15.23	-16.65	23.43	22.04	58.5	26.9	0.65
		Cherry	20	-17.73	-20.88	23.23	21.73	56.6	20.4	0.66
		Rice	21	-22.37	-25.45	23.23	22.04	61.6	16.0	0.66
		Grassland	31	-24.47	-27.99	23.41	21.74	58.4	23.8	0.67
		Barren land	20	-26.91	-31.58	23.14	22.16	43.6	15.5	0.74
2	Spring season	Sugarcane	31	-14.62	-16.56	23.03	21.86	58.7	28.0	0.64
		Wheat	20	-17.37	-18.81	23.03	21.54	56.5	21.2	0.65
		Grassland	31	-25.36	-28.41	23.21	21.54	60.0	28.0	0.67
		Barren land	20	-26.22	-29.09	22.95	21.97	38.7	15.2	0.72
3	Summer season	Sugarcane	31	-14.02	-16.81	23.84	21.96	62.0	26.9	0.63
		Wheat	20	-17.07	-19.81	23.13	21.64	52.3	26.4	0.64
		Grassland	31	-24.50	-28.00	23.31	21.65	54.0	26.8	0.69
		Barren land	20	-26.14	-29.11	23.05	22.07	38.7	15.2	0.72

Table 2: Maximum (Max) and minimum (Min) values of N_a, *LAI*, *PWC* and *h* for three seasons

			Areal density (N_a)		*LAI* (m^2/m^2)		*PWC*		*h* (m)	
S.No	*SAR* images	Land cover class	Max	Min	Max	Min	Max	Min	Max	Min
1	Autumn season	Sugarcane	804.23	671.53	5.927	5.434	0.738	0.726	1.650	1.649
		Cherry	631.52	449.43	5.330	4.400	0.692	0.676	1.260	1.248
		Rice	3014.35	1479.71	3.740	2.400	0.657	0.619	0.780	0.770
		Grassland	20000.00	3720.93	3.170	0.500	0.269	0.175	0.211	0.209
2	Spring season	Sugarcane	725.5	570.95	5.260	4.620	0.861	0.764	1.673	1.607
		Wheat	615.42	518.45	5.510	4.870	0.634	0.622	1.267	1.242
		Grassland	22016.53	6087.89	2.680	2.360	0.540	0.120	0.210	0.209
3	Summer season	Sugarcane	777.47	596.24	5.800	4.850	0.920	0.760	1.661	1.628
		Wheat	588.95	464.26	5.280	4.430	0.627	0.590	1.253	1.252
		Grassland	17933.88	3135.39	2.170	1.220	0.229	0.225	0.196	0.195

Table 1 and these indicates the relative response of green vegetation, surface roughness height and topography towards backscatter coefficient.

The R^2 values in Table 1 indicate a relatively weak correlation between σ_D^0 and m_v for the data collected at all sampling locations. Further, relatively lower correlations (R^2 ~ 0.63 to 0.66) between σ_D^0 and m_v were observed for samples collected from vegetative surfaces in contrast to barren fields (R^2 ~ 0.71 to 0.74) for the three seasons. The grassland represented short sparsely covered grass plants that contributed less towards attenuation of σ_D^0, which resulted in higher correlations (R^2~0.67 to 0.68) for this land area than other vegetated surfaces. The sugarcane covered land for all the three seasons resulted in lower R^2 values, which may be attributed to the fact that sugarcane crop being much larger in height and denser than the other vegetated surfaces and thus produced more attenuation of the σ_D^0 values. The low correlations over the barren land may be attributed to the presence of surface roughness which may have scattered the σ_D^0 in this case.

These observations further corroborates our belief that that σ_D^0 can not be directly related to volumetric soil moisture and the effects of topography (if present), vegetation cover and surface roughness on σ_D^0 need to be considered for further improvement of the sensitivity of backscatter coefficient for accurate retrieval of crop covered soil moisture from *SAR* images. Also, the area was topographically flat; the effect of topography on backscatter coefficient for the estimation of volumetric soil moisture was found to be relatively insignificant and therefore has not been reported here.

Effect of Vegetation: The direct backscatter coefficient (σ_D^0) was refined by reducing the effect of vegetation through implementation of the semi-empirical water cloud model. Backscatter coefficient estimated after minimising the effect of vegetation *via* water cloud model has been

Table 3: Variance explained by the relation between σ^0_{DV} with m_v for the data of three seasons

			Model 1 (*LAI*)	Model 2 (*PWC*)	Model 3 (*h*)
S. No.	*SAR* Images	Land cover class	R^2	R^2	R^2
1	Autumn season	Sugarcane	0.84	0.71	0.68
		Cherry	0.85	0.71	0.68
		Rice	0.86	0.72	0.69
		Grassland	0.86	0.73	0.70
2	Spring season	Sugarcane	0.84	0.72	0.71
		Wheat	0.84	0.72	0.72
		Grassland	0.85	0.74	0.74
3	Summer season	Sugarcane	0.84	0.73	0.73
		Wheat	0.85	0.74	0.74
		Grassland	0.86	0.74	0.75

termed as direct-vegetation corrected backscatter coefficient (σ^0_{DV}). To simplify the water cloud model, three important vegetation descriptors, namely, *LAI*, *PWC* and *h* were used separately resulting into three different models. The range of estimated values of N_a, *LAI*, *PWC* and *h* are given in Table 2, which clearly indicates that sugarcane crop due to their mature stage and thick density of cropping has higher values of *LAI* and *PWC* over other crops. Also, the values of *h* for sugarcane crop are more due to the moist soil and leaf foliage on the soil surface.

The values of coefficients of water cloud model (*i.e.*, *A* and *B*) depend on the type of vegetation descriptor (i.e., *LAI*, *PWC* and *h*). These coefficients were estimated for each descriptor using Quasi-Newton minimisation algorithm by inputting the *in-situ* measured values of *LAI*, *PWC* and *h* individually. The coefficients *C* and *D* were obtained by establishing a regression relationship between σ^0_D and m_v for the barren land.

Once the coefficients were estimated, σ^0_{DV} were computed separately for the three models using Eq. (4). To assess the effect of each vegetation descriptor on backscatter coefficient, regression elimination approach was adopted. This led to identification of a single vegetation descriptor that has maximum impact in weakening of the *SAR* signal. Results of regression between σ^0_{DV} obtained from three models and observed m_v in terms of R^2 values are given in Table 3.

Clearly, a significant increase in R^2 values (Table 3) can be observed over those given in Table 1, for each vegetative cover. This is particularly true in case of Model 1 which utilises *LAI* as the vegetation descriptor. This may be due to the fact that *LAI* is characterised by the density of vegetation in accordance to the size of the leaf that actively participates in weakening of the backscatter coefficient through the vegetation layer [6, 11, 29].

In the present study, the effect of dielectric constant of vegetation on backscatter coefficient was found to be less than that by *LAI*. Similarly, the third vegetation descriptor, *h*, also exhibited the lowest effect on the backscatter coefficient.

The scatter plots between σ^0_{DV} obtained from model 1 and observed m_v for all vegetative surfaces corresponding to autumn season are shown in Figure 2.

Thus, water cloud model with *LAI* as vegetation descriptor showed a significant effect on $\sigma°$ and therefore has been used further for the retrieval of soil moisture.

Retrieval of Soil Moisture Through non Linear Least Squares Method: An empirical model proposed by Dubois *et al*. [22] was used to compute the backscatter coefficient, referred here as (σ^0_{cal}). The model incorporates two key parameters (*i.e.*, surface roughness and the dielectric constant) of the soil. The *rms* surface roughness heights (*s*) were computed mechanically using surface roughness profiler. The σ^0_{DV} computed from the Eq. (4), σ^0_{cal} obtained from Dubois model along with the observed soil moisture ($m_{v_{obs}}$) were input to the least squares method (*LSM*) for the estimation of volumetric soil moisture ($m_{v_{est}}$). The *LSM* derived soil moisture was conceived to be the refined or adjusted soil moisture free from the *in-situ* measurement and calibration errors. For illustration, scatter plots between averaged $m_{v_{obs}}$ and $m_{v_{est}}$ for sampling locations over barren and vegetated

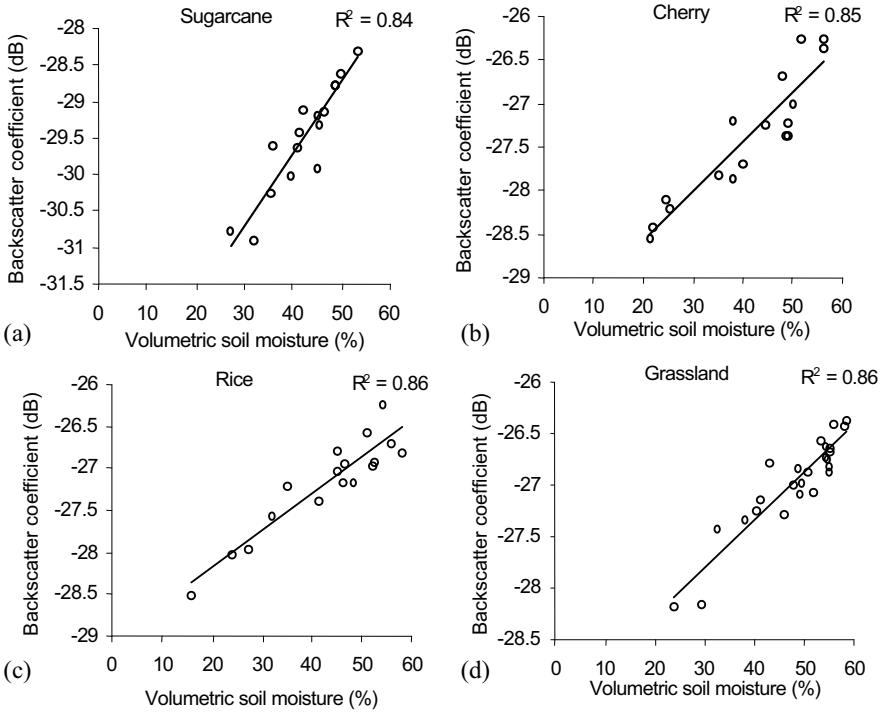

Fig. 2: Scatter plots between σ^0_{DV} and mv for all vegetation classes corresponding to autumn season (N: number of soil sampling locations)

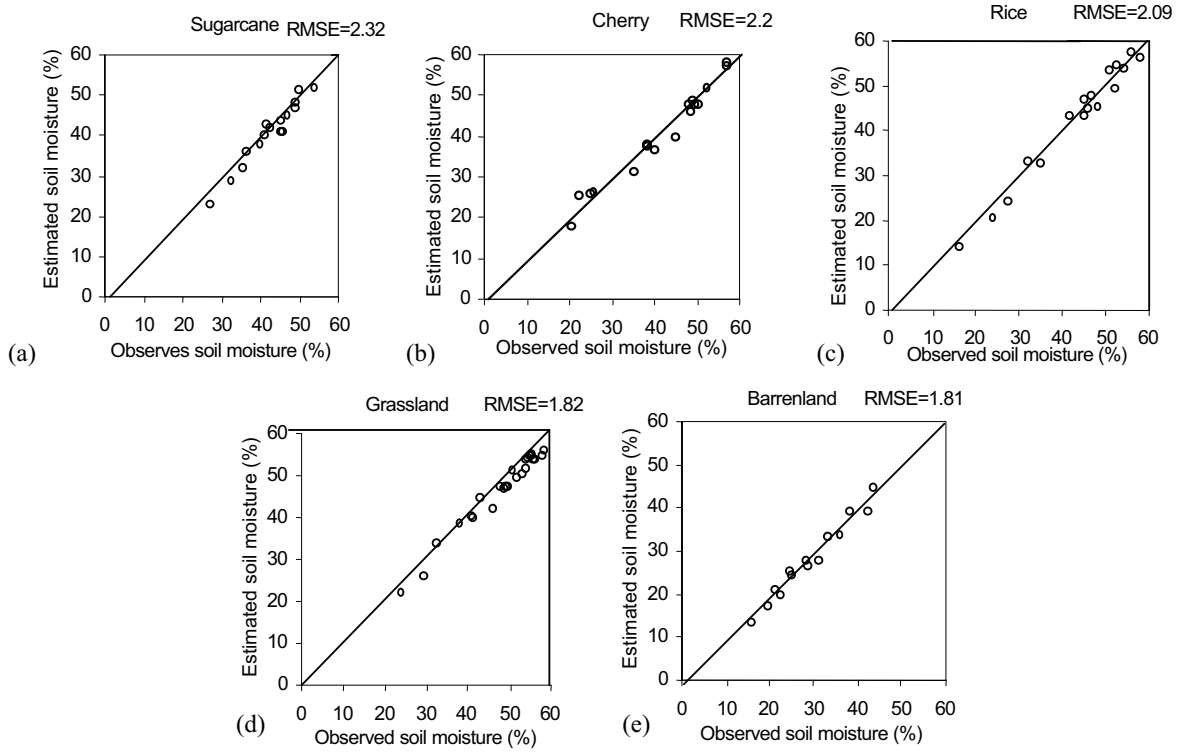

Fig. 3: Scatter plots between $m_{v_{obs}}$ and $m_{v_{est}}$ for all land cover classes corresponding to autumn season (*N*: number of soil sampling locations)

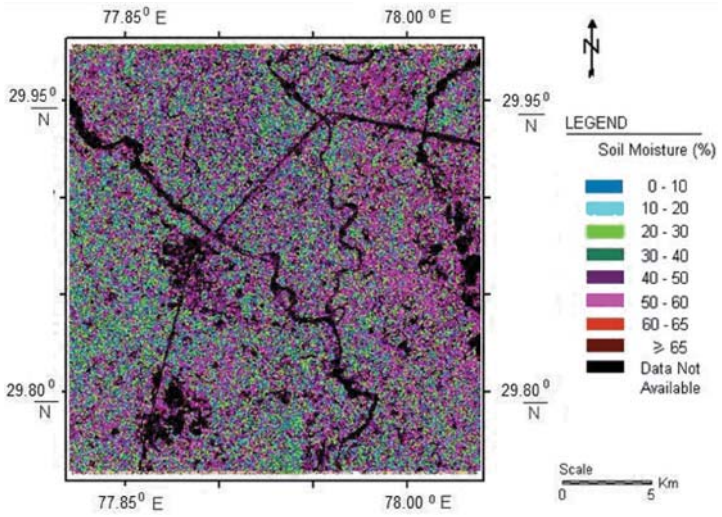

Fig. 4: Soil moisture map of Solani river catchment prepared from *SAR* image acquired in autumn season (*i.e.*, of date 28th July 2003).

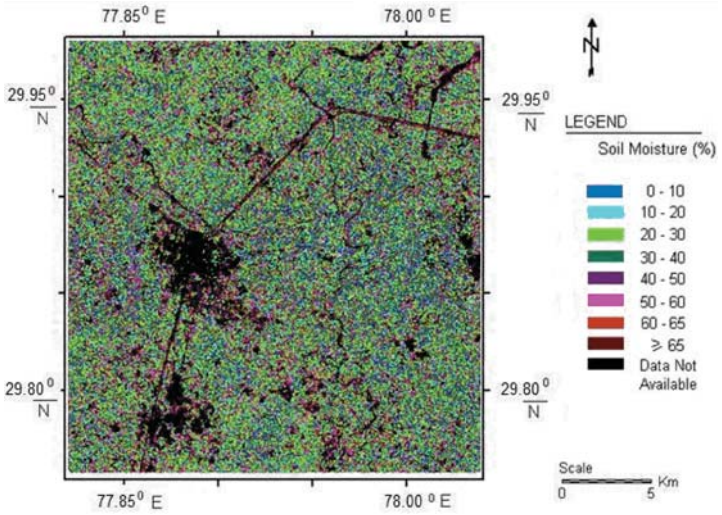

Fig. 5: Soil moisture map of Solani river catchment prepared from *SAR* image acquired in spring season (*i.e.*, of date 29th March 2004).

surfaces corresponding to the autumn season is shown in Figure 3. It can be seen that for all the cases, R^2 values were found to be higher than 0.94, which represent a strong agreement between $m_{v_{obs}}$ and $m_{v_{est}}$. Further, in order to examine the goodness of fit of the data processed in *LSM*, an F-ratio test between $m_{v_{obs}}$ and $m_{v_{est}}$ was also performed at 95% confidence level for all the cases.

Generation of Soil Moisture Maps: Volumetric soil moisture estimated from *LSM* ($m_{v_{est}}$) was regressed with σ^0_{DV} . On comparing the R^2 values (for all models), it can be inferred that relation between backscatter coefficient and the estimated soil moisture *via LSM* (*i.e.*, σ^0_{DV} and $m_{v_{est}}$) is stronger than the relation between direct backscatter coefficient σ^0_{DV} and the *in-situ* observed soil moisture, m_v.

The soil moisture maps generated for the three seasons depict the spatial variations of soil moisture in the study area. The maps thus derived were compared to the actual soil moisture conditions on the concurrent dates of image acquisitions. It is to mention that the night before the date of autumn image acquisition experienced rainfall, which resulted in the increase of soil moisture in most of the agricultural fields within the study area.

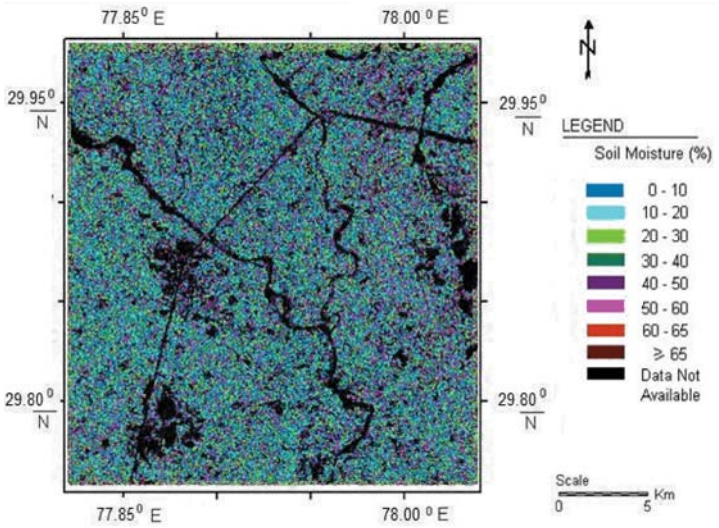

Fig. 6: Soil moisture map of Solani river catchment prepared from *SAR* image acquired in summer season (*i.e.*, of date 3rd May 2004).

This feature is clearly evident in the soil moisture map produced in Figure 4, which reveals that most of the area is covered with 50% to 60% range of the volumetric soil moisture. Similar inferences can also be made for the maps generated for the other two seasons (Figure 5 and 6), which show soil moisture variation from 20% to 30% considering the fact that these two seasons were relatively dry due to the scanty rainfall in the antecedent periods. The soil moisture values at a few locations in the maps of spring and summer seasons have been estimated as more than 50%. This may be attributed to the reason that the barren fields were irrigated up to the saturation level in these seasons as these were being prepared for the cultivation of next crop.

Such soil moisture maps produced from this study for three seasons may be of vital importance and can be used to represent the soil moisture state of the catchment that is a key input for Physics-based distributed storm-event rainfall-runoff soil erosion models. These maps may also find their usefulness for many other hydrological applications such as in planning, designing and scheduling of irrigation systems.

Model Validation: From the maps, the volumetric soil moisture at each pixel can be obtained. In order to further validate the developed approach, an independent sample of data consisting of 20% of sampling locations of barren land and vegetated surfaces in all the three seasons was utilised and compared with the soil moisture values extracted from the maps at the sampling locations. Results reveal that soil moisture may be estimated with a maximum error of ± 10% in all the cases. This independent evaluation further substantiates the fact that the proposed approach can retrieve soil moisture at spatial level from *SAR* images with high accuracy in the catchment of Solani river.

CONCLUSIONS

In this paper, an approach based on semi-empirical water cloud model was developed for the estimation of soil moisture from *ERS*2 *SAR* images by reducing the effect of vegetation on backscatter coefficient. The aim was to simplify the model by minimizing the inclusion of a number of vegetation descriptors in the water cloud model. The study area belonged to Solani river catchment, India. were compared. Amongst the three crop descriptors namely *LAI, PWC* and *h* studied, the *LAI* was found to be the best descriptor in minimising the effect of vegetation on soil moisture retrieval from *SAR* images. Close agreement ($R^2 > 0.95$) between the retrieved soil moisture and the corresponding observed volumetric soil moisture was observed for both barren as well as vegetative surfaces. This clearly demonstrates the applicability of the approach suggested.

The use of a single canopy descriptor (*i.e.*, *LAI*) in the water cloud model is the major finding of the present study. Since *LAI* information can now be extracted from optical remote sensing data at spatial level its use in Physics based models shall assist in production of soil moisture maps with high degree of accuracy.

Future research may, however, be targeted to include other *RADAR* configurations (*e.g.*, multi-polarisation and multi-incidence angle) in a variety of field conditions before the use of present approach can be recommended at the operational level.

REFERENCES

1. Ulaby, F.T., J. Cihlar and R.K. Moore, 1984. Active Microwave Measurement of Soil Water Content, Remote Sensing of Envir., 3: 185-203.
2. Attema, E.W.P. and F.T. Ulaby, 1978. Vegetation modelled as a water cloud, Radio Sci., 13(2): 357-364.
5. Baghdadi, N., C. King, A. Chanzy and J.P. Wingneron, 2002. An empirical calibration of IEM model based on SAR data and measurements of soil moisture and surface roughness over bare soils. International J. Remote Sensing, 23(20): 4325-4340.
6. Moran, S.M., D. Christa, Peters-Lidard, M.W. Joseph and S. McElroy, 2004. Estimating soil moisture at the watershed scale with satellite-based radar and land surface models, Canadian J. Remote Sensing, 30(5): 805-826.
7. Jackson, T.J., R. Bindlish, A.J. Gasiewski, B. Stankov, M. Klein, E.G. Njoku, D. Bosch, T. Coleman, C. Laymon and P. Starks, 2004. Polarimetric Scanning Radiometer C and X Band Microwave Observations During SMEX03. In: Proceedings IEEE International Geoscience and Remote Sensing Symposium, 1: 321-324.
8. Prévot, L., I. Champion and G. Guyot, 1993. Estimating surface soil moisture and leaf area index of a wheat canopy using a dual-frequency (C and X bands) scatterometer, Remote Sensing of Envir., 46: 331-339.
9. Lang, R. and H. Saleh, 1985. Microwave inversion of leaf area index and inclination angle distributions from backscattered data, IEEE Transactions on Geoscience and Remote Sensing, GE-23: 685-694.
10. Sano, E.E., A.R. Huete, D. Troufleau, M.S. Moran and A. Vidal, 1998. Relation between ERS-1 synthetic aperture radar data and measurements of surface roughness and moisture content of rocky soils in a semiarid rangeland. Water Resource. Res., 34(6): 1491-1498.
11. Bindlish, R. and A. Barros, 2002. Subpixel Variability of remotely sensed soil moisture: An inter-comparison study of SAR and ESTAR, IEEE Transactions on Geoscience and Remote Sensing, 40: 326-337.
13. Holah, N.T., N. Baghdadia, M. Zribib, A. Bruandc and C. Kinga, 2005. Potential of ASAR/ENVISAT for the characterization of soil surface parameters over bare agricultural fields, Remote Sensing of Envir., 96: 78-86.
14. Rao, Y.S., A.K. Singh, S. Sharma and G. Venkataramani, 2007. ENVSAT ASAR Polarimetric Data for soil moisture mapping, PolInSAR workshop 2007, held at Frascati, Italy.
15. Srivastava, H.S., P. Patel Y. Sharma and R. Navalgund, 2009 Large-Area Soil Moisture Estimation Using Multi-Incidence-Angle RADARSAT 1 SAR Data, IEEE Transactions on Geoscience and Remote Sensing, 47(1): 2528-2535.
16. Roo De, R., Y. Du, F.T. Ulaby and M.C. Dobson, 2001. A semi-empirical backscattering model at L-band and C-band for a soybean canopy with soil moisture inversion, IEEE Transactions on Geoscience and Remote Sensing, 30(4): 864-872.
17. Ulaby, F.T., R.K. Moore and A.K. Fung, 1986. *Microwave remote sensing, active and passive; Volume III: From Theory to Applications*. Artech House, Norwood, MA.
18. Champion, I. and G. Gyot, 1992. Generalised formulation for semi-empirical radar models representing crop backscattering, Proceedings of the 5th International Colloquium, Physical Measurements and Signatures in Remote Sensing Courchevel, *ISPRS-ESA_CNRS-INRA-IFREMER, ESA* SP-319: 269-272.
19. Capstick, D.R., 1998. The application of ERS-2 SAR data in the prediction of sugar beet and potato crop yields, Department of Geography, University College London, unpublished, M.Sc Thesis.
20. Clevers, J.G.P.W. and H.J.C. Van Leeuwen, 1996. Combined use of optical and microwave remote sensing data for crop growth monitoring, Remote Sensing of Environment, 56: 42-51.
21. Wigneron, J.P., P. Ferrazzoli, A. Olioso, P. Bertuzzi and A. Chanzy, 1999. A simple approach to monitor crop biomass from C-band radar data, Remote Sensing of Envir., 69: 179-188.
22. Dubois, P.C., J. Van Zyl and T. Engman, 1995. Measuring soil moisture with imaging radars, IEEE Transactions on Geoscience and Remote Sensing, 33(4): 915-926.
23. Bennet, J.M. and L. Mattson, 1989. Introduction to Surface Roughness and Scattering, Optical Society of America, Washington D.C.
24. Lee, J.S., 1983. Digital Image Smoothing and the Sigma Filter. Computer Vision, Graphics and Image Processing, 24: 255-269.

25. Laur, H., P.J. Meadows, J.I. Sanchez and E. Dwyer, 1993. ERS-1 SAR Radiometric Calibration, *Proceedings of the CEOS SAR Calibration Workshop, ESTEC, Noordwijk, The Netherlands*, ESA Publication WPP-048: 257- 281.
26. Lakhankar, T., H. Ghedira, M. Temimi, A.E. Azar and R. Khanbilvardi, 2009. Effect of Land Cover Heterogeneity on Soil Moisture Retrieval Using Active Microwave Remote Sensing Data. Remote Sensing of Environment, 1(2): 80-91.
27. Fung, A.K., Z. Li and K.S. Chen, 1992. Backscattering from a randomly rough dielectric surface, IEEE Transactions on Geoscience and Remote Sensing, 30(2): 356-369.
28. Hoekman, D., L. Krn and E. Attema, 1982. A multilayer model for radar backscattering by vegetation canopies, Proceedings of IEEE International Geoscience and Remote Sensing Symposium, (IGARSS'82), Munich, Germany.
29. Paris, J.F., 1986. The effect of leaf size on the microwave backscattering by corn, Remote Sensing of Envir., 19: 81-95.
30. Dobson, M.C. and F.T. Ulaby, 1986. Preliminary evaluation of the SIR-B response to soil moisture, surface roughness and crop canopy cover, IEEE Transactions on Geoscience and Remote Sensing, 24(4): 517-526.